Arc root dynamics in the context of lightning strikes to aircraft

Vincent Andraud, R Sousa Martins, Clément Zaepffel, Romaric Landfried, Philippe Teste, Philippe Lalande

Arc root dynamics in the context of lightning strikes to aircraft

V Andraud[1], R Sousa Martins[1], C Zaepffel[1], R Landfried[2], P Testé[2] and P Lalande[1]

[1]DPHY, ONERA, Université Paris Saclay, F-91123 Palaiseau, France
[2]Laboratoire GeePs, CNRS UMR8507, Université Paris Saclay, CentraleSupélec, 91190 Gif-sur-Yvette, France

E-mail: rafael.sousa_martins@onera.fr

Abstract

During lightning strikes to aircraft, there is a displacement of the impacted area on the aircraft's surface and the dynamic of the arc root is a key to understanding and predicting the damage produced on the aircraft skin. This work aims at studying experimentally this dynamic with a new method of producing sweeping arcs based on a stationary arc and an electromagnetic launcher propelling aeronautical test samples. The experiments are also achieved with a wind tunnel that blows the arc on the test sample for comparison. After a description of the previous experiments of arc root displacement and a distinction between the cathodic and anodic emission processes, this paper characterizes the arc root physical properties with direct visualization through high-speed cameras and electric measurements for different initial conditions. The results are separated by the arc root polarity and discussed to give an insight into the influence of the experimental conditions on the interaction between the electric arc root and the test sample during swept-stroke. It is shown that for a cathodic arc root, the nature of the displacement – continuous or jumping – highly depends on the current level and the speed of the relative motion between the electric arc and the test sample. For an anodic arc roots, the variations of these parameters provoke jumping modes of displacement with different characteristics.

I. Introduction

I.1. Lightning strikes to aircraft

When an aircraft is struck down by lightning, the impact point forms an arc root, capable of sweeping or leaping along the metallic cover [1]. Several numerical [2, 3] and experimental [4, 5] works have characterized the electrical, thermal damage, and mechanical stresses resulting from the impact on the aircraft's surface. However, the most recent computational models, incorporating complex MHD models [6, 7] and turbulent instabilities [8] still predict severe conditions for reattachment, conflicting with available experimental observations [1, 9]. Yet, these codes currently do not account for the role of arc root electric emission processes, despite experimental observations indicating substantial variations in arc root behaviour and displacement based on polarity.

Additionally, no experimental work has successfully reproduced significant in-lab lightning arc swept-strokes to provide accurate and quantitative results of arc root displacement. This lack of experimental data currently poses challenges for optimizing the protections for the new generation of aircraft composed of reinforced carbon fiber and featuring new geometries. The present work aims to establish an experimental database that addresses these scientific needs through the implementation of an in-lab lightning swept-stroke experiment. The experimental results are presented through two different perspectives: first part of this work focused on characterizing the arc column during its elongation due to the swept-stroke and was published in [10]. The second part of this work is dedicated to the study of the arc root displacement and is presented within the scope of this paper.

I.2. Arc root displacement in literature

While there is relatively little literature available about the experimental displacement of arc roots issued from lightning channels, other applications present a substantial literature where the physical phenomenon occurring are better analyzed and understood. Indeed, there is an important literature for two main applications where the arc root motion is the key preoccupation for efficiency issues: the circuit breakers [11] and the plasma torches [12, 13].

In these applications, the characteristic arc lengths differ by one or two orders of magnitude from the electric arcs generated by the developed lightning generator, their length rarely exceeding a few cm. First, this addresses a scale problem: a small distance between the two arc roots greatly impacts the physical mechanisms responsible for their displacement. It is shown in [14] that the metal vapor and gas ablated from the electrodes are providing strong jets that are likely to be bent under the influence of the magnetic field coming from the arc current. These jets are heating the other electrode in a favored direction and affect the physical processes for the establishment of an arc root thus greatly influencing the displacement of the arc roots by enhancing their mutual influence. In swept-stroke experiments, the electric arcs are meter-scaled and thus the displacement of the arc root is supposedly not affected by the presence of the opposite arc root.

The most studied configuration for the displacement of an electric arc is the displacement between parallel electrodes consisting of metallic bars [14-18]. The arc moves forward due to the Laplace force coming from his self-induced magnetic field or enhanced by an external one. The main observation on the displacement mode – for arc current up to 1 kA and several mm of distance between the rails – are that the cathodic arc root has a continuous mode of displacement whereas the anodic arc root moves forward along the rails by jumping. Depending on the experimental conditions, the cathode arc may present a jumping pattern of displacement as well and there might be multiple – up to four – distinct anodic arc roots [14, 15, 18 – 20]. In these configurations, the cathodic arc root was either preceding the anodic arc root [15, 16] or not [14, 18]. Secker and Guile [19] also classifies four types of cathodic arc roots tracks that matches different types of displacement: discontinuous (jumping mode), regular (continuous with tracks of a regular size due to relatively low dwell time), sticking (continuous with tracks of important size due to relatively important dwell time) and high speed (continuous with thin tracks). Then the displacement modes were associated with the following parameters:

1. Current intensity: as the current increases, the displacement goes from sticking to regular, from regular to high speed and then from high speed to discontinuous even if does not seem to have an influence on the velocity of arc root displacement.
2. The materiel: it is shown in [14] that a refractory material with a low work function is likely to present a discontinuous mode. This mechanism will be discussed in the cathodic arc root subsection.
3. The inter-electrode distance: it was observed that as this distance increases in the range from 0 to 50 mm, the displacement of the arc roots is faster and the mode of displacement is becoming discontinuous. The speed however presents a saturation threshold.

There are few works of electric arc experiments where the arc roots are displaced due to the relative motion of the electrodes with speeds reaching several tens of m/s. Testé *et al.* [21] present a device consisting of a spinning cylindrical electrode by the use of a drill. The other electrode is a disc concentric with the rotational axis of the spinning electrode and is maintained fixed. A maximum relative speed of 40 m/s was reached for an arc root moving at the extremity of the disc. It was observed for a current of 100 A that the cathodic arc root tracks were either continuous or partially continuous and the anodic arc root tracks were discontinuous – corroborating the previous experimental results. More interesting, it was shown that the

anodic arc root was able to move at the limiting speed of the device – 40 m/s whereas the cathodic arc root was only able to move at tens of mm/s to be maintained and avoid arc extinction. This behavior was attributed to the drastic conditions of heating and electric field thresholds for a cathodic spot to emit electrons so that the arc root cannot be faster than the temperature propagation in the surface of the material. Dobbing and Hanson [9] is a reference that presents a configuration similar to our required performances with a linear movement of the electrode expelled at a speed up to 72 m/s. This reference proposes experimental data for arc voltage drops for reattachment over painted surfaces, skip distance values between two arc roots in discontinuous modes and dwell time values of the arc root on a specific point for bare metal and carbon fibers. It also evokes a different behavior of the electric arc above and below the moving electrode and the difference of displacement mode between the cathodic and the anodic arc roots.

The primary objective of this paper is to investigate the displacement of the arc root during the swept-stroke. In order to recreate the pertinent conditions for an experimental study and establish a database meeting scientific requirements, this study employs a test-bed facility previously developed and detailed in two recent papers: a current-regulated lightning arc generator [22] and an electromagnetic launcher [23]. These devices are integrated to replicate an indoor swept-stroke experiment. Section II outlines the experimental setup employed to reproduce the swept-stroke phenomenon in the laboratory. Section III delves into the phenomenology of the arc root motion during the swept-stroke, providing details on different emission processes for both a cathode and an anode. The experimental results concerning the characterization of the arc root displacement, obtained through optical and electrical diagnostics, are presented in Section IV. Subsequently, Section V explores the impact of experimental parameters on the physical and dynamic characteristics of the arc root displacement during the swept-stroke phenomenon.

II. Experimental setup

II.1. Description of the test equipment

The apparatus utilized to simulate a lightning swept-stroke in the laboratory includes a lightning arc generator, an enhanced railgun electromagnetic launcher, and a wind tunnel. This experimental setup is identical to the one presented in [10]. To provide clarity, we briefly recapitulate the main characteristics below.

The lightning arc generator, can generate electric arcs longer than one metre, with a continuous current adjustable within the range of 200 to 600 A, adhering to the C* standard aeronautical lightning waveform outlined in Eurocae ED-84 [24]. The railgun equipment can propel aeronautical test samples weighing between 100 and 250 g at speeds ranging from 40 to 80 m/s within a 2 m acceleration distance. Experiments involving the railgun propelling aeronautical test samples through an electric arc are denoted as RGE in this study. The wind tunnel, powered by a 15 kW DELTALAB motor, enables flow monitoring for velocities up to 70 m/s. Experiments employing the wind tunnel to direct the electric arc onto the test samples are also referred to as WTE in this context.

The test samples comprise plates of aeronautical aluminium alloy 2024-T3 with a thickness of 0.4 mm, wrapped and stiffened around a resin pattern of NACA 0012 airfoil with a chord length of either 200- or 400-mm. Current measurements utilize a PEM CWT AC CWT60LF probe, while voltage measurements employ North Star PVM-1 and Lecroy PPE5KV reference voltage probes. The swept-stroke phenomenon is captured by two high-speed cameras (HSC) – Phantom V711 models from Vision Research with a CMOS sensor of 1280 × 800 pixels and 20 µm². One camera is positioned perpendicular to the axis of projectile

movement in the railgun experiment and perpendicular to the flow direction in the wind tunnel experiment, adjusted at the sample's height.

For a more detailed account of the experimental coupling between the arc lightning generator and the railgun or wind tunnel, as well as the implementation of diagnostics, please refer to [10].

In figure 1, the diagram of the RGE and a picture of a swept-stroke with a high-speed camera (HSC) are presented. In figure 2, the diagram of the WTE and a picture of a swept-stroke are presented.

(a)

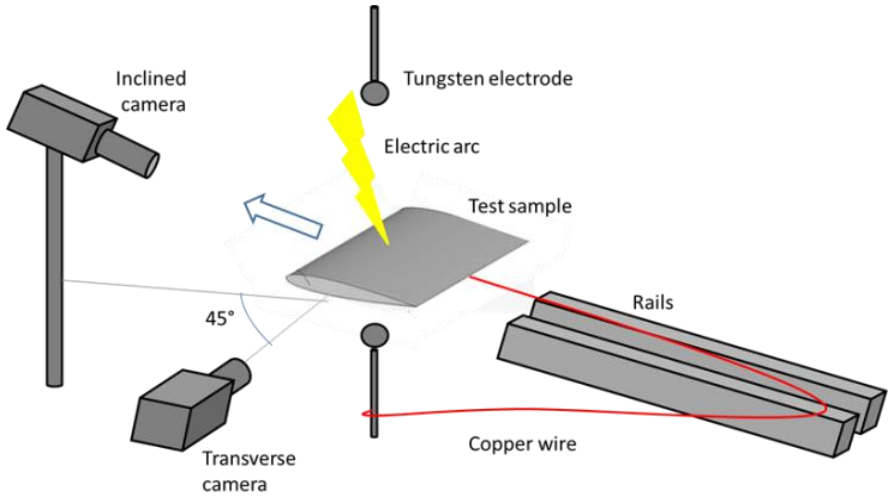

(b)

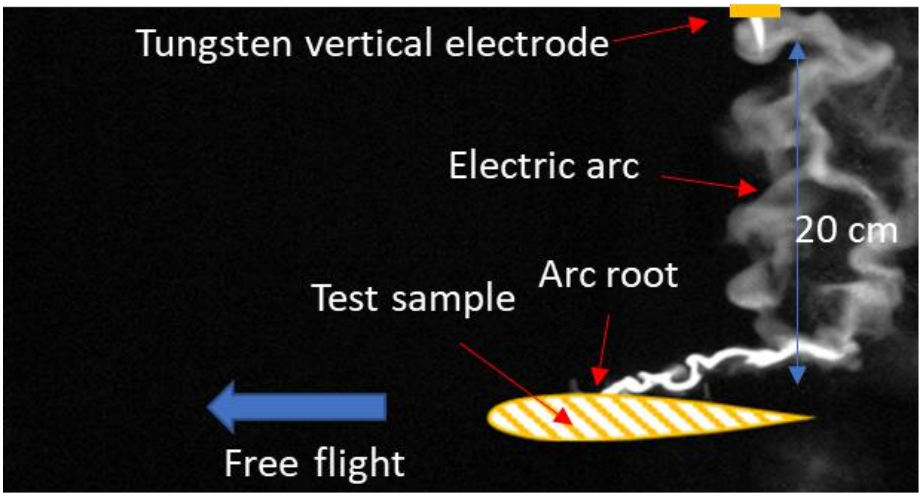

Figure 1. (a) Diagram of the railgun setup with the two cameras and (b) picture of the swept-stroke taken with HSC for RGE.

(a)

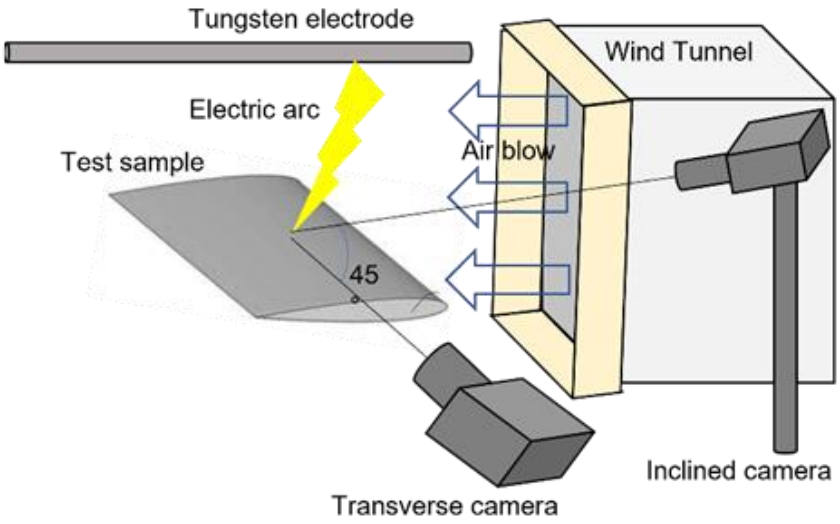

(b)

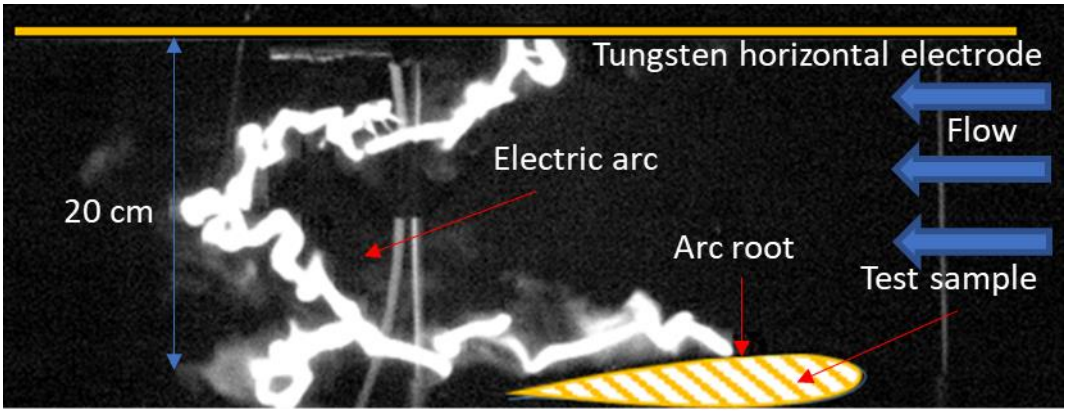

Figure 2. (a) Diagram of the wind tunnel setup with the two cameras and (b) picture of the swept-stroke taken with HSC for WTE.

III. Phenomenology of the arc root displacement during the swept-stroke

III.1. Swept-stroke phenomenology and arc root displacement

As described in [10], the RGE and WTE are composed of five phases: the arc ignition, the static phase, the swept-stroke, the arc elongation and the arc extinction. The voltage and current of the electric arc during these phases are respectively depicted in figure 3 and figure 4. As the displacement of the arc root on the test sample surface occurs during the swept-stroke, this study only focuses on this phase.

This phase is triggered with the first attachment of the arc channel on the material test sample and is characterized by an abrupt voltage drop of hundreds of volts (visible at instant 17.6 ms on figure 3(a)). Then, in the RGE, one arc root is stalled on the upper motionless electrode and the other arc root is involved in complex processes of dwelling and reattachment on the moving test sample whereas in the WTE, both arc roots are free to move: one moves on the test sample whereas the other moves on the horizontal test electrode. Multiple arc extinctions and arc formations occur due to magnetic loop effects or to the

reattachment of electric arc roots on the test sample. This might provoke occasional and sudden voltage drops. These phenomena are visible through the saw-tooth shape of the voltage waveform during the swept-stroke phase presented in figure 3(b) for RGE. The global elongation of the arc during this phase generates the global increase in arc voltage despite the occurrence of some measured abrupt and marked voltage drops. As can be seen in figure 4, the current amplitude is maintained at 400 A +/- 40A during this phase thanks to the active regulation circuit of the lightning generator that is described in [22].

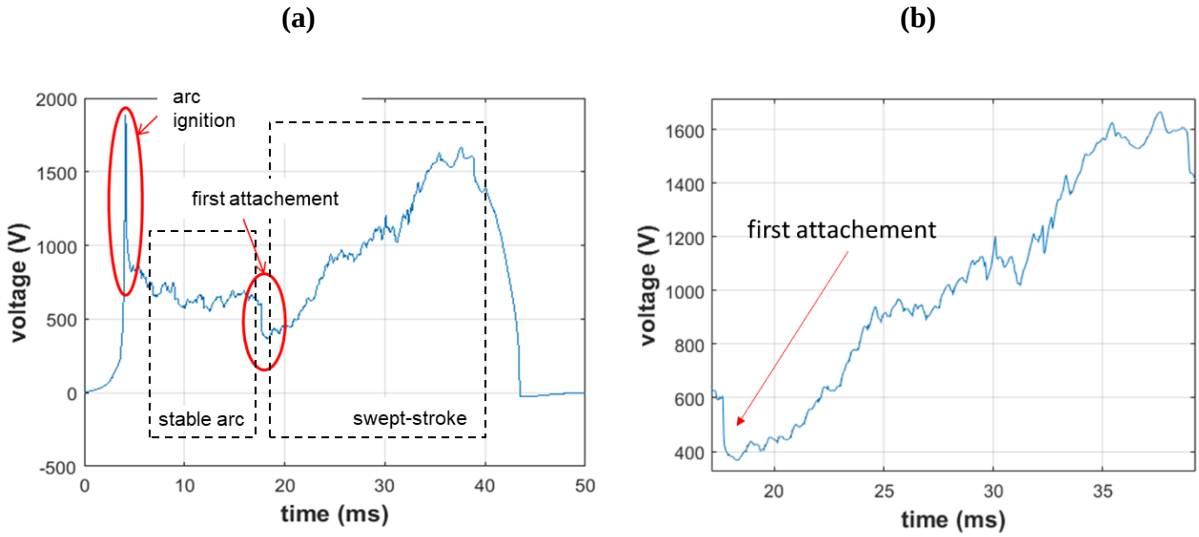

Figure 3. Arc voltage waveform for the RGE; (a) For the entire arc lifetime. (b) For the swept-stroke phase.

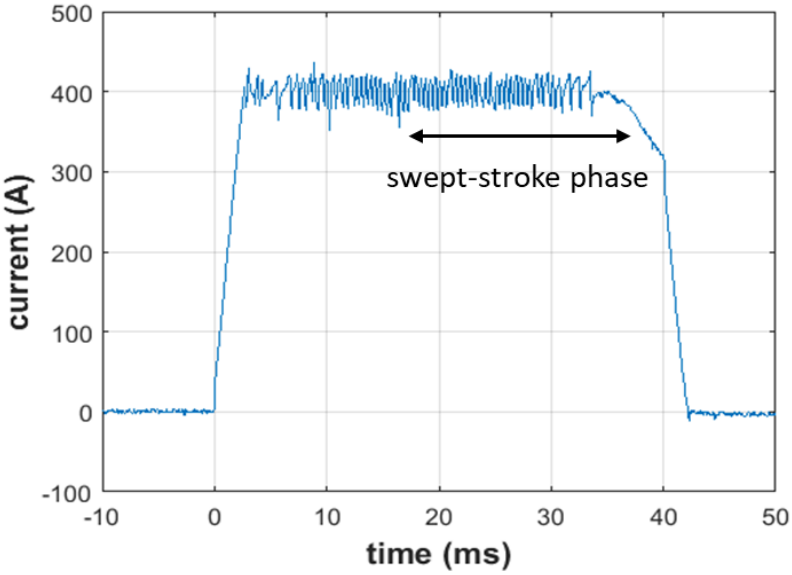

Figure 4. Arc current waveform for the RGE.

According to the literature, it is presupposed that a competition between electromagnetic and hydrodynamic forces drives the swept-stroke phenomenon, as represented in figure 5, even if the role of the arc root emission process is not considered [6, 7]. Figure 5(a) represents the initial instant of the swept-stroke. As the lightning arc attaches on the metal skin of the test sample, the arc root is ensuring the physical interface between the arc channel and the metal through electronic emission processes (positive ions emission or electrons emission depending on the metal polarity). This arc channel maintains the DC current flowing

through the electric arc. The arc channel is subject to the air flow, which is often modelled with a Blasius profile [6, 7] even though a turbulent flow is expected to overlap [8]. The no-slip condition of the profile imposes that the arc root is not affected by the flow as the laminar boundary layer is larger than the arc root [25]. It results in the arc channel stretching to maintain the electrical contact as described in figure 5(b). When the arc increases in size, as its internal electric field is kept constant [26], its electric potential increases as well. Then, depending on the arc root emission process, the local flow and electromagnetic fields, two different processes can occur: a continuous sweeping (the arc root is gliding on the metallic surface) or a discontinuous sweeping (the arc root is jumping on the metallic surface).

During a continuous sweeping, as depicted in figure 5(c), due to local emission of charged particles the metal area at the direct vicinity of the arc root is subject to a high local electric field and to an increased Joule effect. These mechanisms might trigger electrical emission processes from this area and thus modify the arc root expansion. As the arc channel is pulling the arc root in the flow direction, the emitting sites at the outer radius opposite to the flow direction are subject to less intensive electric field and are likely to tail off. This resulting in the continuous arc motion of the arc root as described in figure 5(d): the arc root is moving and the arc channel integrity is maintained.

During a discontinuous sweeping, as depicted in figure 5(e), the electric potential of the arc channel increases, and the distance between a point of the arc channel and the test sample might be momentarily shortened due to the local hydrodynamic and electromagnetic constraints. Consequently, another distinct emitting site may be formed, short-circuiting a section of the existing arc channel and the arc root. A new section of arc channel is formed: the electric current flows through this new path and the old portion of the arc channel and the arc root extinguish as shown in figure 5(f).

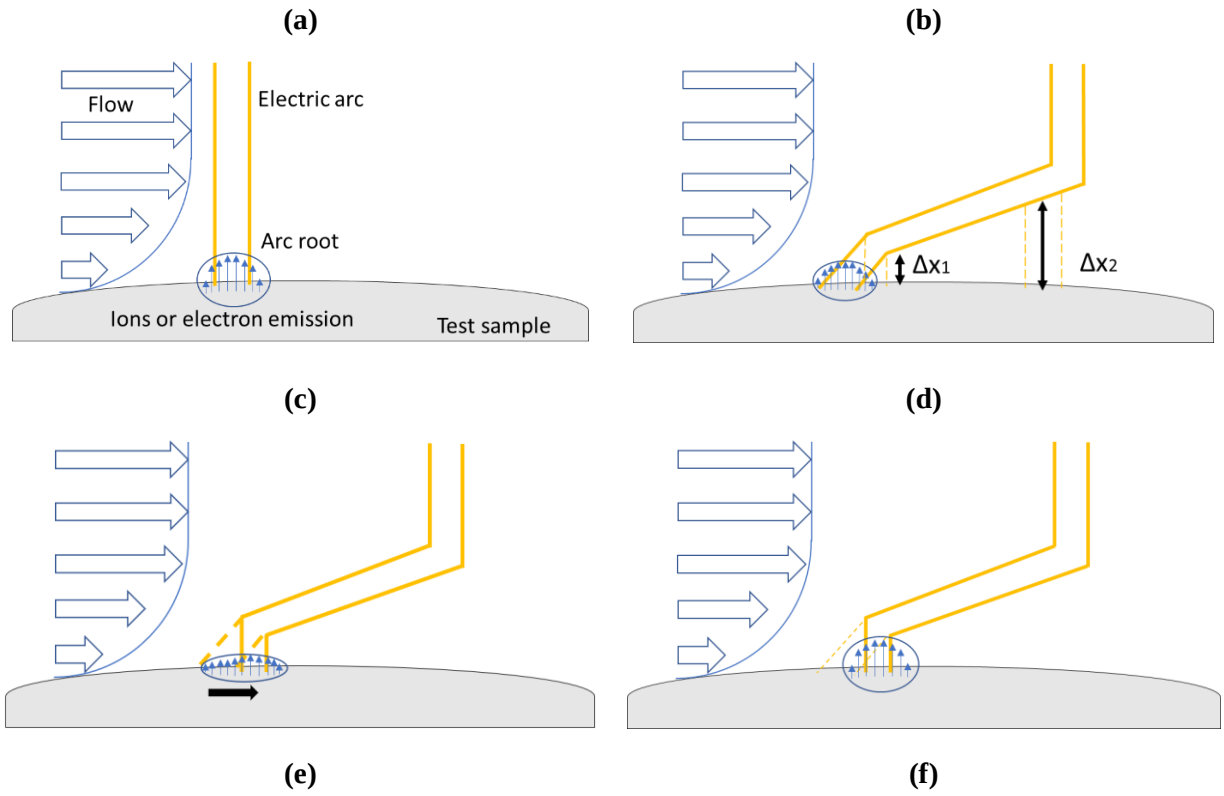

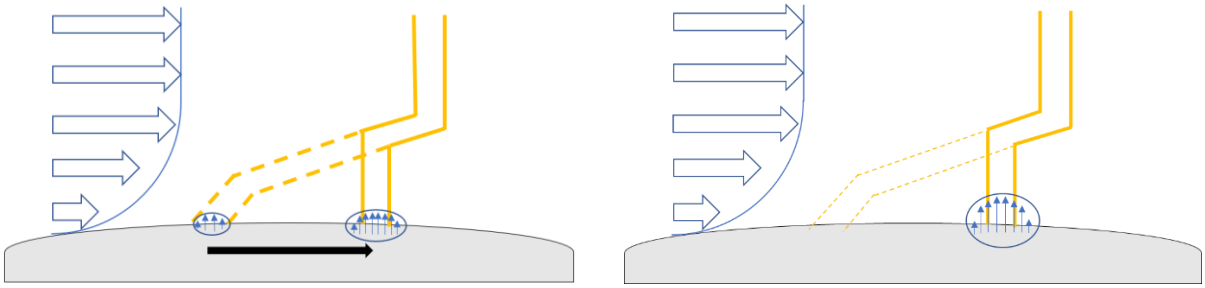

Figure 5. Different mechanisms of swept-stroke in the metal test sample reference frame for the RGE or WTE (a) An electric arc attaches on the sample. (b) The arc is blown and stretched by the flow of the relative wind. (c) For a continuous mode the arc root is displaced through a process of formation and (d) Extinction of the emitting sites at the close vicinity of the existing arc root. (e) For a discontinuous mode, a distinct emitting site is formed to shorten the arc channel, a breakdown creates a new channel and (d) provokes the extinction of a portion of the channel and the corresponding arc root.

As it will be presented in the next sections, the mode of sweeping – continuous or discontinuous – highly depends on the arc root polarity.

III.2. Emission processes and dynamics of the cathodic arc root

The cathodic root is the plasma sheath between the region of the solid metallic conductor and the gas at the cathode. By extension, the cathode fall region includes the cathode surface and the thin layer of electrode vapor and gas around it. The cathode has a very important role since it regenerates the charged particles of the electric arc and so maintains the discharge. The cathode requires the flow of positive ions and electrons are extracted from it. It is commonly accepted that the cathode emission dominates the displacement of the entire arc column caused by self-induced magnetic field or exterior forces [27].

The main features of this cathode fall region arc are the presence of a voltage drop between 8 and 20 V occurring over very short distances from the metal surface [28]. Thus, the electric field in this region has a higher order of magnitude that the one in the arc channel: whereas the field in the arc column is around 10 V/cm, it might exceed 10^7 V/cm in the cathode fall region. The typical current density of this region is also over several order of magnitude than the density in the column (10^4 to 10^5 A/cm^2 for refractory cathode material, 10^6 to 10^7 A/cm^2 for non-refractory cathode material [29] and 10^2 to 10^3 A/cm^2 in the arc column).

A cathodic spot has to be able to emit electrons and receive positive ions to maintain the arc current. This emission is possible mainly through Thermionic emission – dependent on the surface temperature and for refractory materials [30] – or Field emission – dependent on the surface electric field [31].

Then the production of ions in the sheath is explained by two main processes:

1. The electrons emitted are accelerated by the large local electric field of the cathode fall region and produce ions at the end of the region by successive collisions.

2. Thermal ionization processes in the high temperature gas at the edge of the sheath respecting the Saha equation and the local thermodynamic equilibrium (LTE).

This theoretical development gives a basis to explain the different observed modes of arc displacement. As it was observed in Cui *et al.* [14], cold cathodes proved to have a continuous and slow arc root displacement whereas thermionic cathodes had either a continuous but faster arc root displacement or a discontinuous one under the same operating conditions. The continuous movement of cold cathodes is explained by the predominance of field effect emission to establish new electrons emitting sites. A region of space charge

from ionized metal is therefore required and the movement is limited by the diffusion of metal vapor. It results in a forward continuous motion of the cathodic root as metal vapor is formed at the vicinity of the arc root. This motion is observed and presented through a sequence of HSC photos in figure 6.

(a)

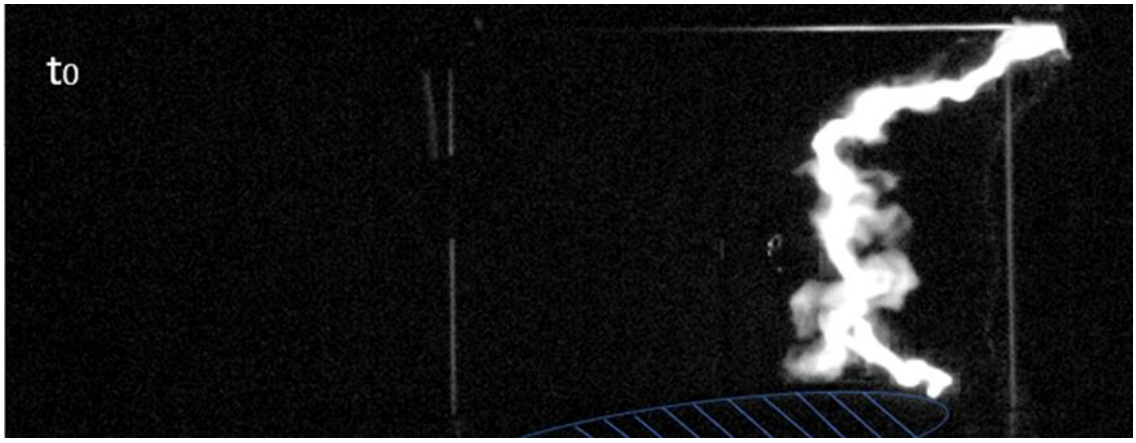

(b)

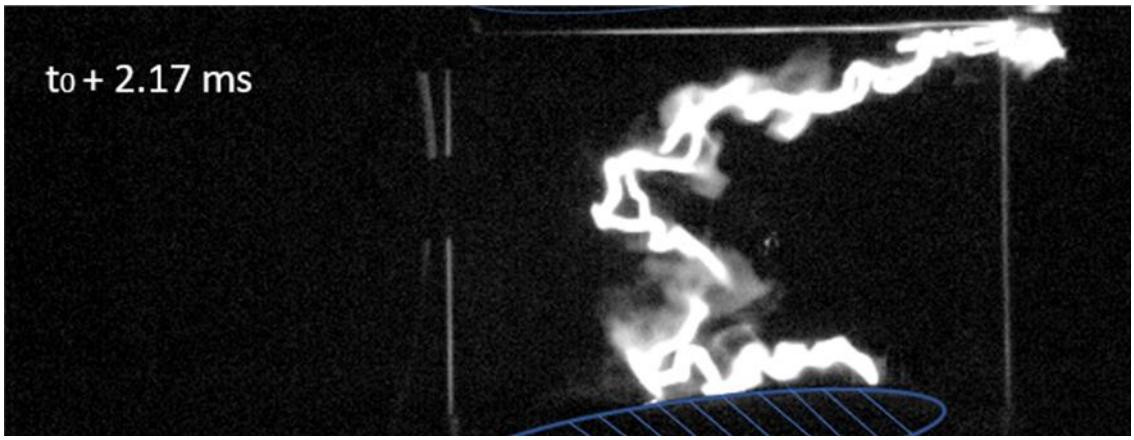

(c)

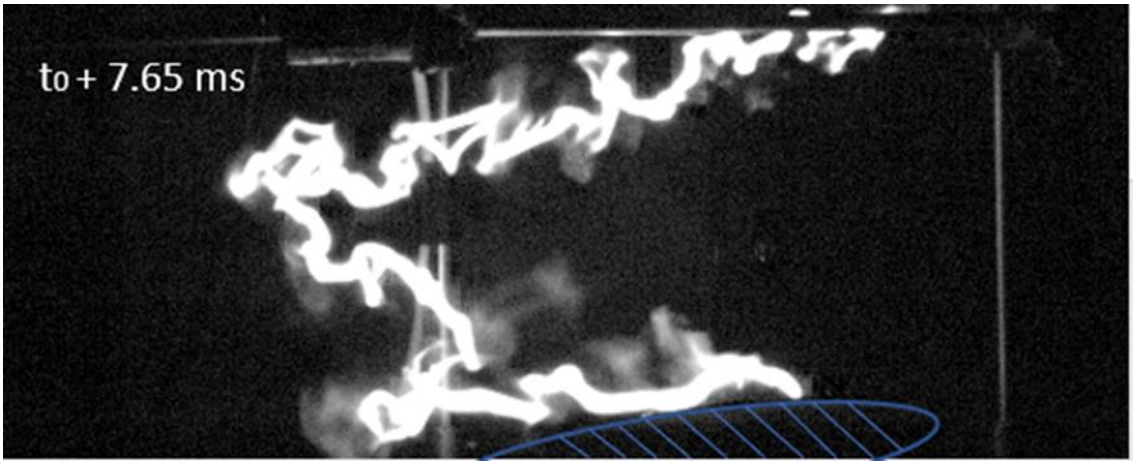

(d)

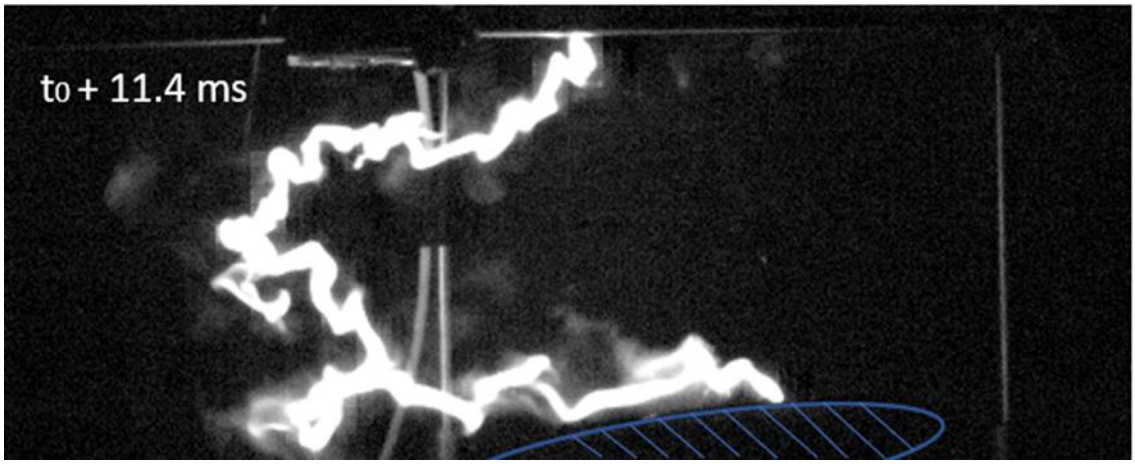

Figure 6. Successive images of a swept-stroke with a continuous mode for a cathodic arc root for WTE.

Figure 7 presents the impact points and the arc root tracks formed by the passage of a cathodic arc root. It shows that the arc root does not only present a continuous movement: depending on the initial conditions, partial discontinuous modes have also been observed during the different experiments.

(a) **(b)**

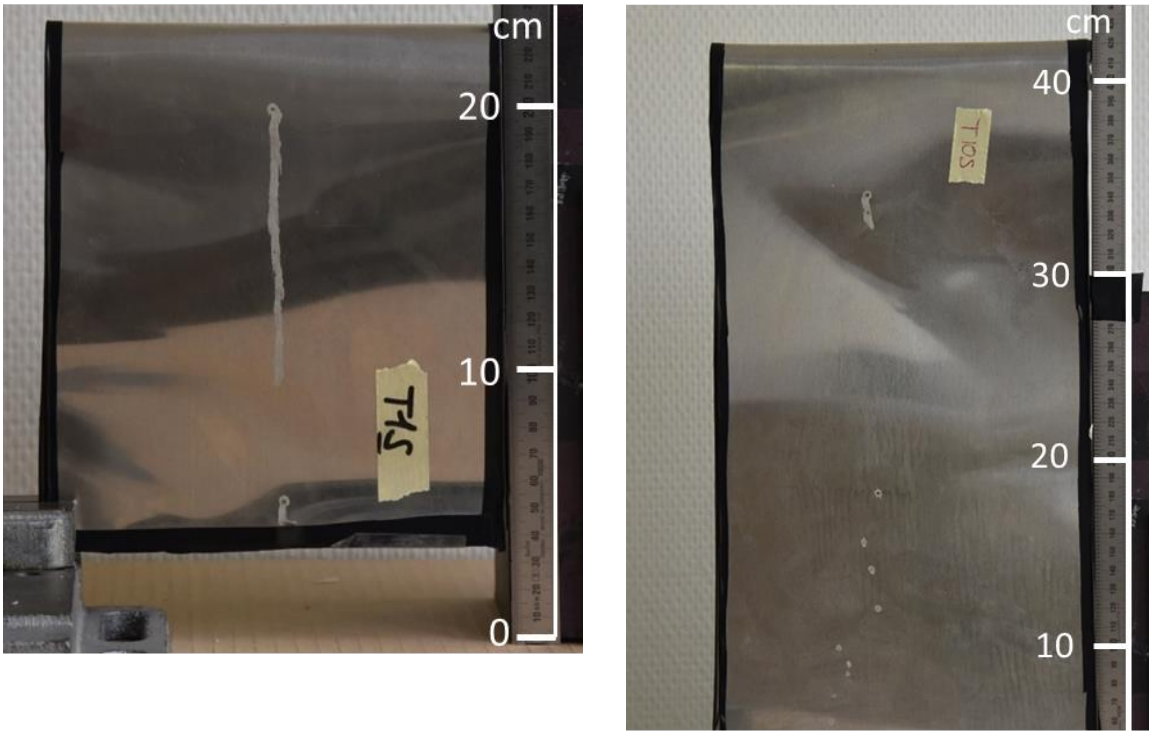

Figure 7. Presentation of different kinds of track left by a cathodic arc root – (a) continuous track and (b) jumping tracks.

III.3. Emission processes and dynamics of the anodic arc root

The anodic root is the plasma sheath between the region of solid metallic conductor and the gas at the anode. By extension, the anode region includes the anode surface and the thin layer of electrode vapor and gas around it. Its role is to preserve the current continuity. The anode cannot emit positive ion. Instead, the current is carried by electrons entering it. Thus, as no charge emission conditions are required, the establishment of an anodic arc root is less restrictive that the cathodic one [28].

The main features of this anode fall region arc are the presence of a voltage drop between 1 and 10 V occurring over very short distances from the metal surface due to a space charge region. This space charge is due to an important concentration of electrons. The current density, unlikely to the cathodic spot, is close to the one in the arc column – 10^2 to 10^4 A/cm^2 [32].

However, if ions are not emitted from the anodic material, they are emitted in the anodic sheath area to sustain the electric arc. There are two emission processes:

1. Thermal ionization processes in the high temperature gas at the edge of the sheath respecting the Saha equation.

2. The electrons entering the sheath are accelerated by field effects and are able to ionize the gas in the sheath. However, this field effect is less predominant than the thermal ionization for atmospheric arcs [33].

Thus, the movement of the anodic spot is most governed by thermal processes than field processes so that the establishment of a new anodic arc root is less dependent on the vicinity of an existing anodic spot which could explain a jumping mode of displacement. McBride and Jeffery [11] also noted that the anodic arc root is more likely to be affected by an additional pressure coming from a venting process than the cathodic spot, supposedly due to the absence of governing emission process. This jumping mode displacement is shown in figure 8 through a series of HSC photos showing the formation of a new arc spot and the extinction of an arc channel portion resulting in a jumping mode of displacement. Figure 9 shows the impacts points left on the test sample after the passage of the anodic arc root. It is worth noticing that, contrary to the cathodic arc root, the jumping mode is the only mode of displacement observed for the anodic arc root.

(a)

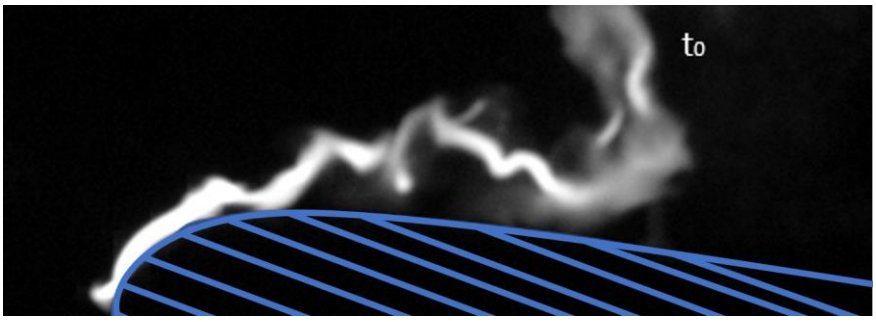

(b)

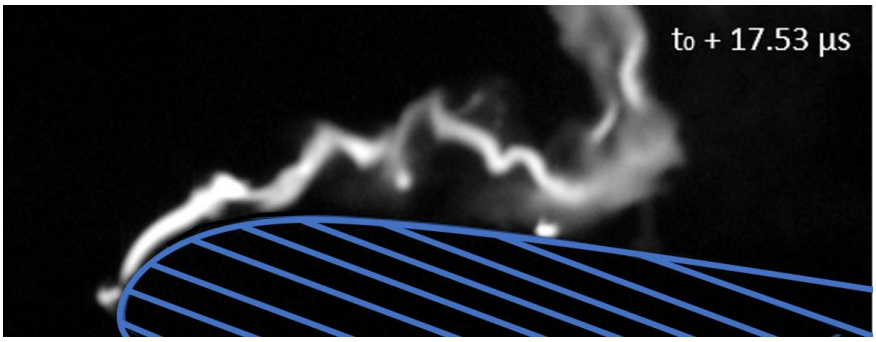

(c)

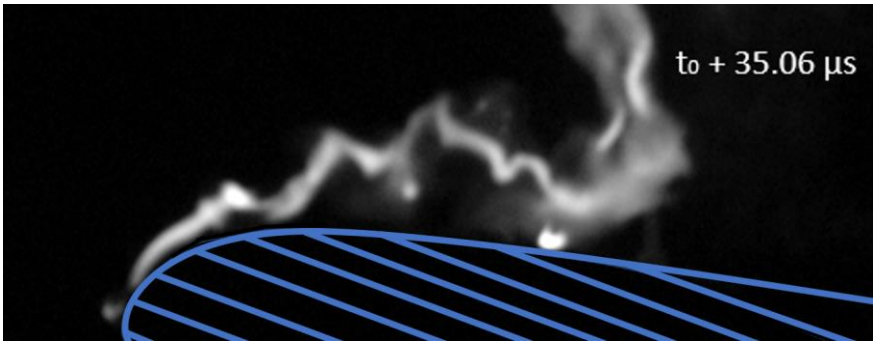

(d)

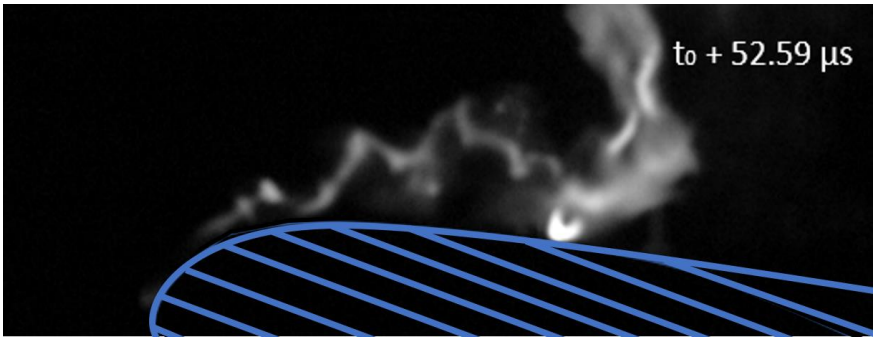

(e)

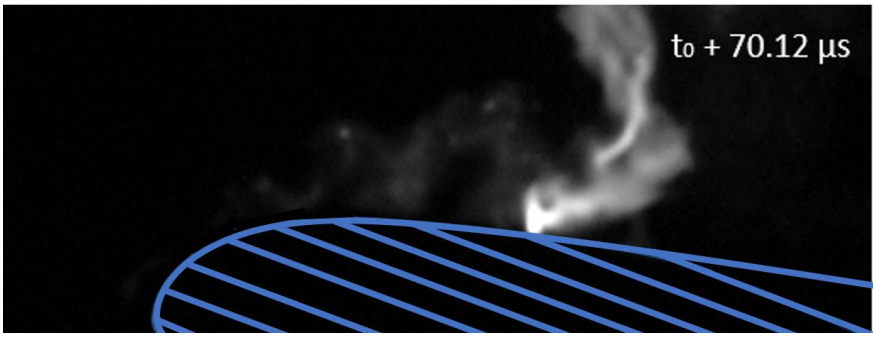

Figure 8. Successive images of a swept-stroke with a discontinuous mode for an anodic arc root for RGE.

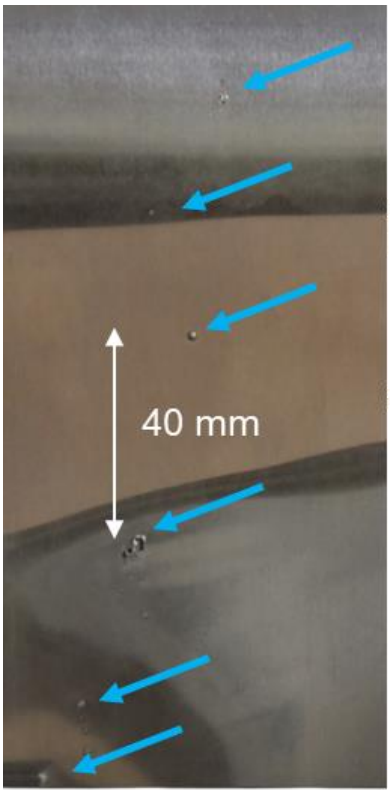

Figure 9. Presentation of impacts on the test sample for an anodic arc root.

IV. Experimental Results

The aim of this work is to establish an experimental database for the arc root dynamics during the swept-stroke and to understand the influence of the dataset parameters. The objective is to analyse the effects of arc current, the relative speed between the electric arc and the test sample, the polarity of the test sample and finally the relative motion system (Railgun or Wind tunnel facilities). The effects of the distance between the electrodes and the length of the test sample can be found in [25], which focuses on how these parameters influence the properties of the arc channel. As the arc root displacement involves different complex multi-physical mechanisms, its study is carried out by varying the input parameters and measuring, by a set of defined observable quantities, its behavior to give a database that will help to interpret the predominant mechanisms occurring. The analyzed quantities are various:

1. dwell time of an arc spot
2. skip distance between two arc spots
3. arc voltage drop occurring during reattachment
4. diameter and number of the impacts left on the test sample by the arc root
5. relative speed of the sweeping cathodic arc root

The results are compiled from approximately 60 shots varying the different initial parameters. The arc current intensity is set at three different values: 200, 400 and 600 A. The relative speed between the test sample and the air flow varies between 40 and 60 m/s. The relative motion system is either RGE or WTE and the arc root polarity is either cathodic or anodic.

The results are given in the form of column charts with error bars: every column averages the measured value of a given physical quantity over three to four repetitions of a specific configuration. Every configuration is defined by a set of the different parameters current intensity, relative speed, mode of

displacement and polarity. Concerning the relative speed in the case of RGE, the relative speed represents the average speed obtained over the three or four repeated experiments. For a given relative speed value, the maximum difference between the repeated experiments of the same configuration is 2 m/s which account for a maximum discrepancy of 5 %. For every column, the error bar gives the minimum and the maximum value of the measured quantity for all the experiments of a specific set of parameters.

IV.1. Dwell time

The dwell time is the time between the formation and the extinction of the same arc root. As these instants of formation and extinction are directly measured with the cameras, their estimation is limited by the interval between two pictures, which is 17.53 µs for the RGE and 15.87 µs for the WTE. The experimental results of dwell time depending on the different dataset parameters are presented in figure 10. It can be observed from the error bars that the dwell time presents a high variability for the cathodic arc root.

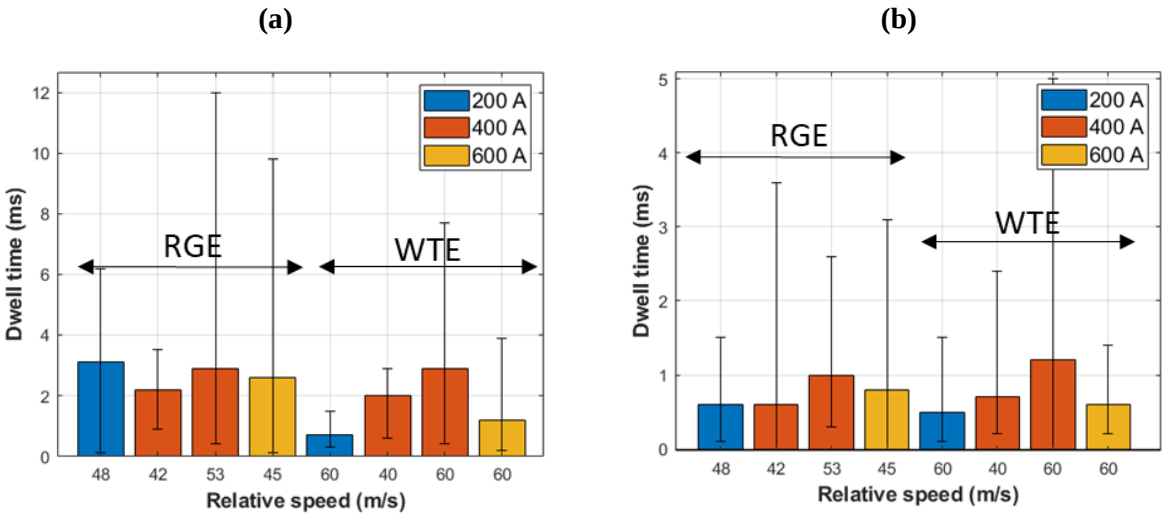

Figure 10. Dwell time evaluation for (a) cathodic arc roots and (b) anodic arc roots

IV.2. Skip distance

The skip distance is the distance between two impact spots and is measured directly on the sample after the test. However, it might occur that different arc roots coexist during the swept-stroke. The experimental results of skip distance depending on the different dataset parameters are presented in figure 11.

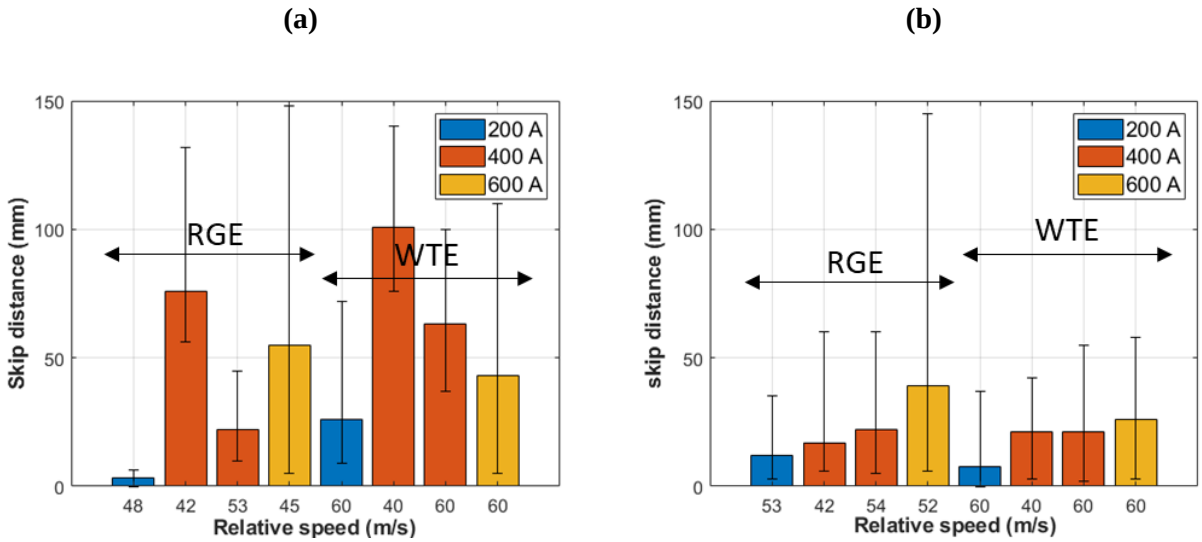

Figure 11. Skip distance evaluation for (a) cathodic arc roots and (b) anodic arc roots

IV.3. Arc voltage drop

When an arc column and an arc root are extinguished due to a reattachment, there is a voltage drop in the arc voltage. This drop corresponds to the voltage of the free arc column and to the electrode voltage fall from the extinguished arc root. Even though the formation of another arc root ultimately compensates the electrode fall. This arc voltage drop value is important since it is also the image of the arc power when it is multiplied by the operative current and it gives complementary information on the real arc length in addition to the 2-D visualization. Indeed, neglecting the cathodic and anodic voltage fall, the arc voltage is supposed to be proportional to the total length of the arc channel. However, voltage drops also occur when an arc loop of the free arc column is short-circuited by the formation of a new path of current. Then, if such a phenomenon occurs during a reattachment, the measured arc voltage drop is composed by the voltage drop due to the arc root reattachment and by the one triggered by the extinction of the arc loop. To recognize the nature of the arc voltage drop, the voltage waveform measurements are synchronized with the transverse camera. The experimental results of arc voltage drop depending on the different dataset parameters are presented in figure 12.

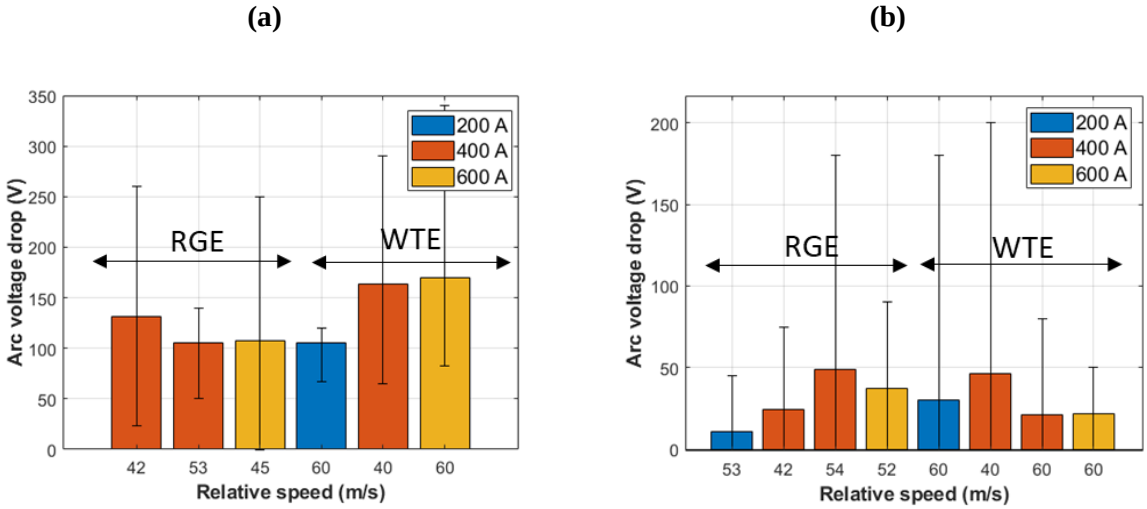

Figure 12. Arc voltage drop evaluation for (a) cathodic arc roots and (b) anodic arc roots.

IV.4. Size and Number of the impacts

The estimations of size and the number of the impacts are made counting and measuring directly the different tracks on the test sample after the experiments.

When the electric arc strikes a point of the surface, this point presents a circular shape whose diameter represents the damages on the structure as a consequence of the different radiative and heat flux mechanisms at the arc root. It is interesting to note that even for a given current level and in the case of a jumping mode for cathodic arc root, the impacts look different between cathodic and anodic arc root, as can be observed in figure 13. The experimental results of impact diameter depending on the different dataset parameters are presented in figure 14.

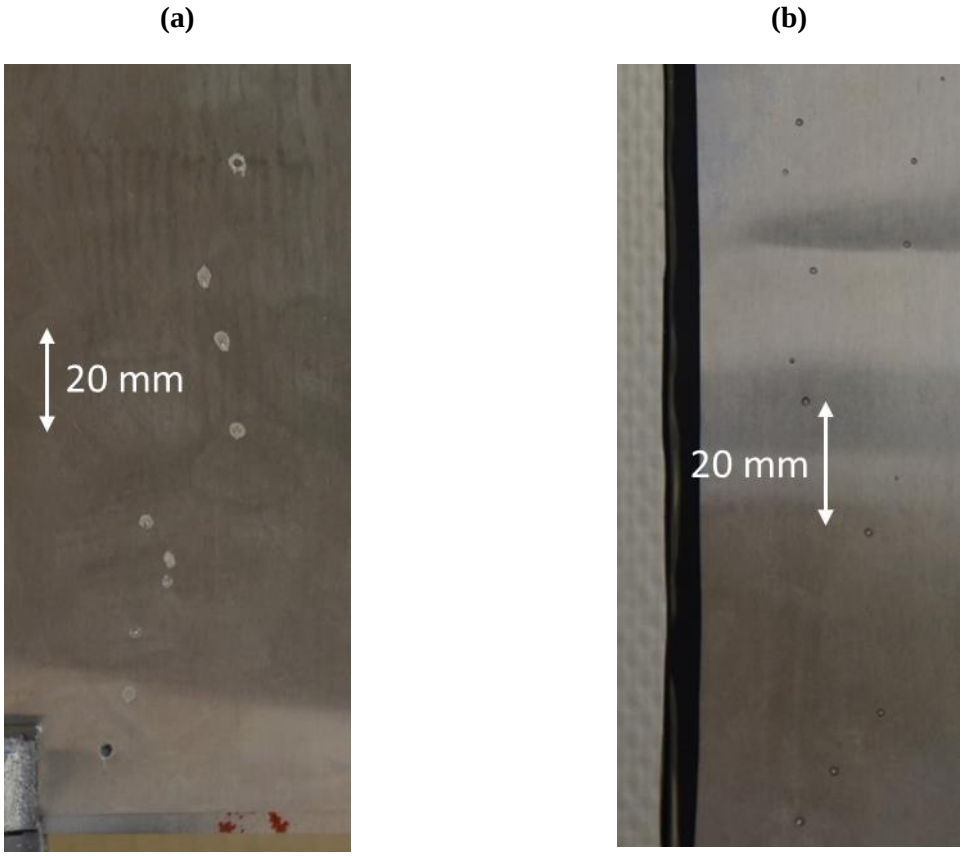

Figure 13. Multiple impacts left by a cathodic arc root (a) and an anodic arc root (b) for 400 A.

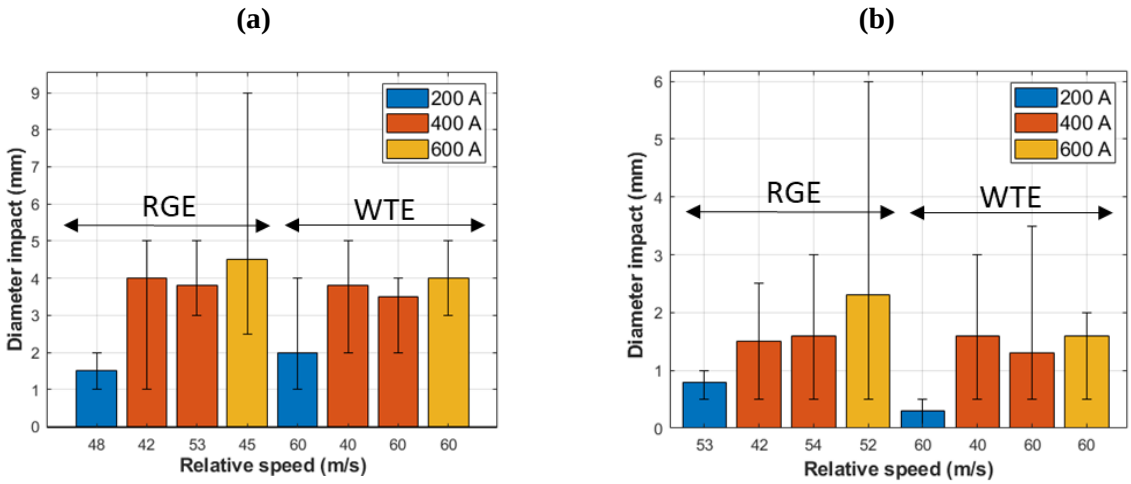

Figure 14. Impact diameter evaluation for (a) cathodic arc roots and (b) anodic arc roots

In general, cathodic arc root spots are more marked with a surrounding circle of barely melted aluminum whereas anodic arc root spots are less marked and do not present this characteristic. It is commonly accepted that these cathodic marks reflect the higher current density of the cathodic spot due to its role of providing electrons to the arc channel to maintain the discharge. The experimental results of number of impacts depending on the different dataset parameters are presented in figure 15.

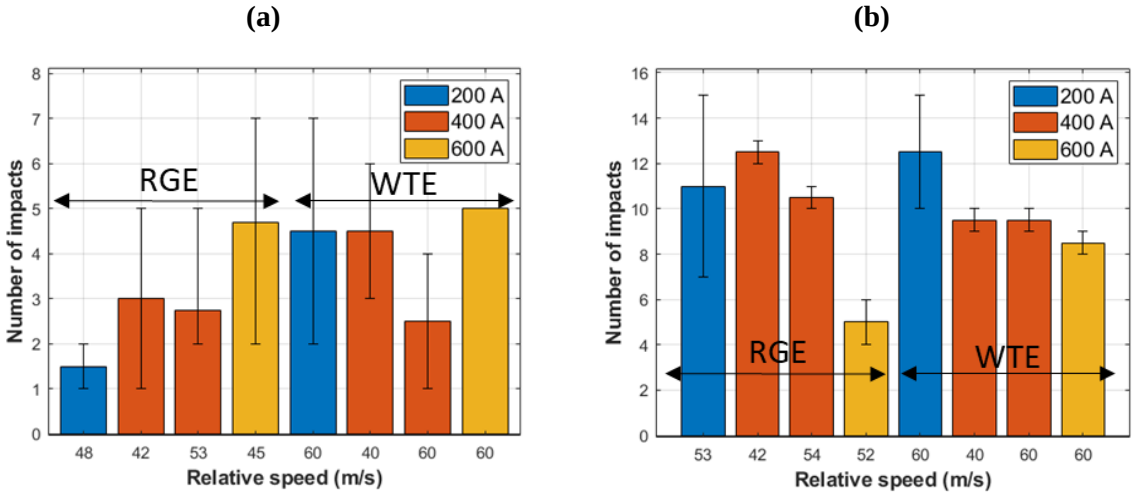

Figure 15. Number of impact evaluation for (a) cathodic arc roots and (b) anodic arc roots

IV.5. Relative velocity of the cathodic arc root

As described in section III, the cathodic arc root presents a continuous displacement for most of the registered experiments. Examples of arc root tracking are presented in Cui *et al.* [14] and Mc Bride and Jeffery [11] using optical fibers or fast recording camera. In our experiment the arc root is tracked resorting the images recorded by the HSC perpendicular to the direction of projectile motion and airflow and an image recognition software.

However, in the RGE, the projectile velocity has to be removed from the measure of the arc root velocity to consider a relative speed. The projectile speed measurement is made at the muzzle exit of the rails and the maximum speed drop evaluated for the series of experiments is less than 5% in the 704 mm distance of launch recorded by the camera. As discontinuous movements are also partially observed, some experiments of cathodic arc root showed several different continuous movements occurring successively and thus

several arc root tracking can be recorded in the same experiment. In this case, the resulting relative speed is averaged over all the mean speeds of the tracked arc root.

It is also interesting to mention that for some records of tracking for the RGE, the arc root is able to move even faster that the projectile considering absolute velocity for a part of the sweeping motion. In this case, the continuous track left by the passage of the sweeping arc root present a V-shape. In the WTE, the cathodic arc root is never observed to be faster than the arc column channel: the arc root is always lagging behind the arc channel in the airflow direction and this result in a standard straight lined continuous track left on the test sample. These different tracks are shown in figure 16. This difference of behavior is complicated to interpret but definitely shows a difference of arc root behavior between the two configurations.

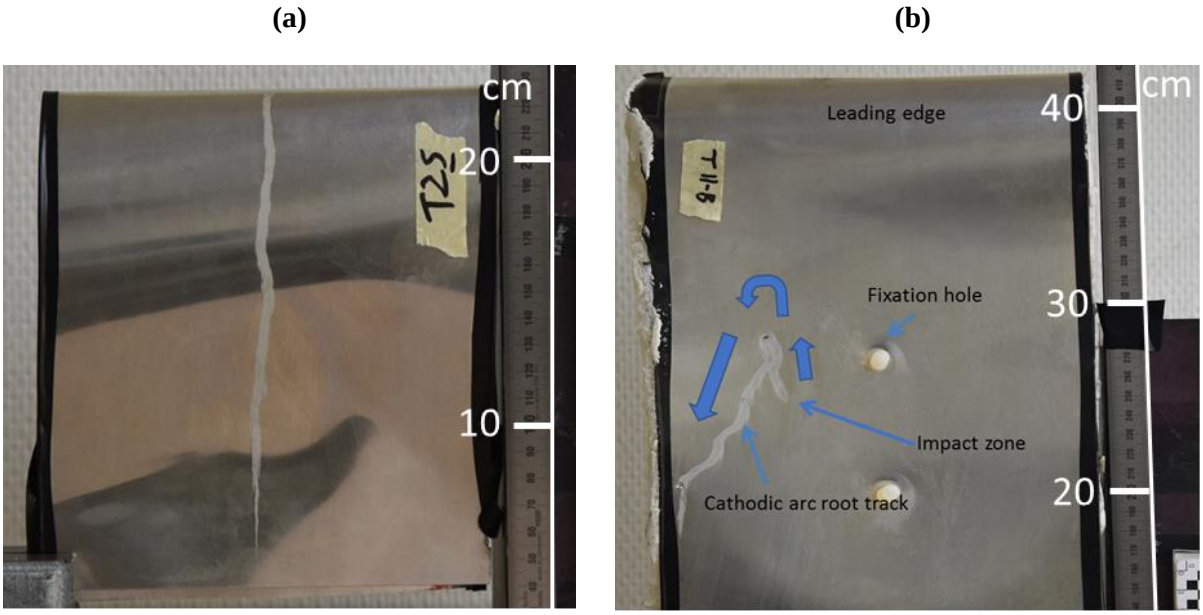

Figure 16. Images of different geometry of sweeping cathodic arc root continuous tracks: (a) straight lined track and (b) V-shaped tracks.

An example of a typical arc root speed evolution during an experiment is given in figure 17 for RGE. In this example, the test sample has a speed of 50 m/s and the relative speed is defined by the difference between the test sample speed and the arc root speed in the frame of the laboratory referential. The relative speed becomes negative at around 6 ms: it means that the arc root is displacing even faster that the test sample in the motion direction at this moment. In this example, the arc root relative speed drops all along the swept-stroke but this is not always observed.

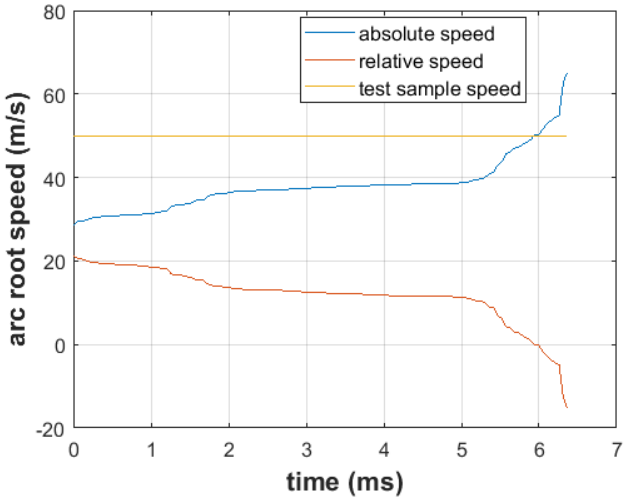

Figure 17. Arc root speed during a Railgun experiment.

The experimental results of cathodic arc root mean speed depending on the different dataset parameters are presented in figure 18.

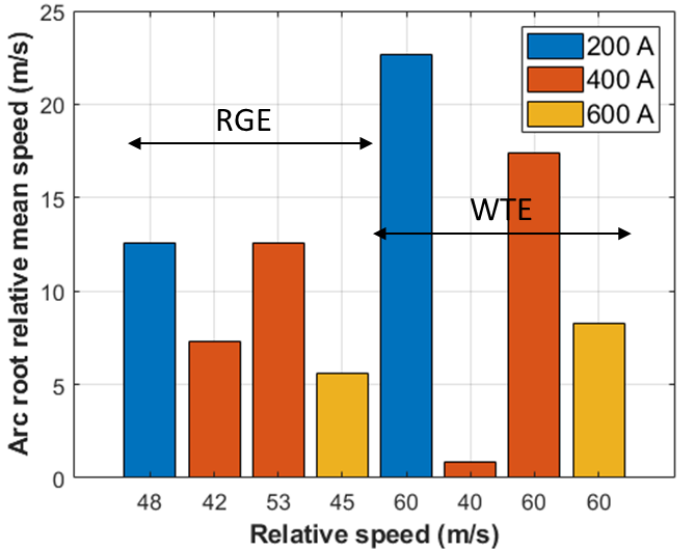

Figure 18. Cathodic arc roots mean speed evaluation.

V. Discussion

V.1. Summary of parameters variations

Tables I and II present the main trends observed for cathodic and anodic spots during the swept-stroke with a comparison between RGE and WTE. They summarize the main difference observed for the behavior of cathodic and anodic spots between the RGE and the WTE. A simple ascending or descending arrow (↗ or ↘) represents an augmentation or a reduction of the measured parameter value between 20 % and 100 % when the input parameter varies from its lowest value to its highest value. A double ascending or descending arrow (↗↗ or ↘↘) presents an evolution that exceed 100 % of variation. A stable arrow (→) represents an

evolution of value within ± 20 % and a simple line (-) represents a lack of information or the impossibility to establish a trend.

TABLE I. Summary of the parameters variations of swept-stroke for cathodic arc spot**.**

RGE / WTE	Dwell time	Skip distance	Arc voltage drop	Size of extinguished arc	Impact size	Number of impacts	Arc root mean speed
Relative velocity ↗	↗/↗	↘↘/↘	→/ -	↘/↘	→/→	→/↘	↗/↗↗
Current ↗	→/-	↗/-	↗/↗	↗/↗↗	↗↗/↗↗	↗↗/-	↘↘/↘↘

TABLE II. Summary of the parameters variations of swept-stroke for anodic arc spot.

RGE / WTE	Dwell time	Skip distance	Arc voltage drop	Size of extinguished arc	Number of impacts
Relative velocity ↗	↗/↗	↗/→	↗/ ↘	→/↘↘	→/→
Current ↗	-/-	↗↗/↗↗	-/-	↗↗/→	↘↘/↘

V.2. Discussions about the cathodic arc root displacement

The results show that the limits between the displacement modes of the cathodic arc root – that can be continuous, partly discontinuous or jumping – are not possible to define clearly with the given criteria since dramatic changes of behavior were observed even for a given setup. Some trends have however been observed for the considered range of input parameters:

A higher relative speed between the electric arc and the test sample fosters a continuous sweeping mode over a jumping mode and this effect is more marked for the WTE than for the RGE. A possible explanation could be the predominance of the field emission for aluminum cathode: if the arc root speed is slower, it has more time to heat locally the electrode material and create a strong amount of metal vapor that increases the local electric field [14]. A strong electric field is likely to stabilize and stall the cathodic arc root despite of the arc channel motion. Thus, it produces reattachments with the extinction of longer arc channels because in the energy balance, the extinction of a longer size of resistive arc channel is required to overcome the high electric field. For a faster cathodic arc root motion, thermal effects do not have enough time to produce the same amount of local metal vapor and the local electric field is weaker and so easier to overcome with the extinction of a smaller and less resistive arc channel. Nevertheless, this explanation is not experimentally verified in the present work. Electric field measurements near the cathodic arc root, as

well as the evaluation of the quantity of metal vapor formed, would need to be implemented to validate this hypothesis.

A higher current of the arc channel seems to favor a jumping mode and this effect is more marked for the RGE than for the WTE. This observation might be explained by two factors. First, a higher current produces a higher magnetic field that creates more important tortuosities. These tortuosities facilitate the rapprochement between the arc channel and test sample surface, increasing the opportunities for a reattachment to occur. Secondly, as aluminum is a cold cathode and the arc root displacement is driven by electric field emission, the higher the current, the higher the required electric field on a spot to sustain the electric discharge. Thus, as the cathode arc root is limited by the diffusion of metal vapor to form charges [20] and locally increase the electric field, a higher electric field requirement needs the formation of more metal vapor and thus slow down the arc sweeping displacement. However, as the electric arc of 600 A is higher in temperature, it is more able to form a new cathodic spot through temperature plus field emission [34] thus explaining the observed jumping pattern. These possible interpretations would need to be verified by measurements of the arc root physical properties – electric field, local temperature and quantities of metal vapor.

V.3. Discussions about the anodic arc root displacement

For the anodic arc root, only a jumping mode is observed. Its behavior remains complex and the experiments implemented do not present marked trends. The following conclusions can be exposed:

For higher relative speed between the electric arc and the test sample, the anodic arc roots present a jumping mode displacement featuring longer dwell times and the formation and the extinction of longer portions of arc channel during a reattachment. The leaps are thus more marked, especially for RGE whereas the leaps and arc channel extinctions are less important for WTE with the relative speed augmentation. This commentary can be related to the observations made in [10] about the arc channel characterization during swept-stroke. It is observed that at low relative speeds for RGE, the arc voltage presents a plateau during the swept-stroke when the arc root is anodic. This voltage plateau is the indicator that the arc reattachment compensates the arc stretching. This observation is consistent with the loose conditions for a metal spot to become an anodic spot in terms of emission processes [27]. The main process driving the arc reattachment is then the minimization of the arc channel resistance which is proportional to the arc length. Therefore, this minimization is ensured by the arc reattachment on the sample. For higher speeds, the interaction of the arc channel with the streamlines unbalances the compensation of the arc stretching with the reattachment of the anodic arc root resulting in increased average dwell time and skip distance.

The current variation provokes effects difficult to understand and compare for RGE and WTE and no real trend is observed, except the increase of size of impact with the current increase due to Joule effect.

VI. Conclusion

A reference experimental database about the arc root displacement during swept-stroke was established resorting to high-speed imaging and electrical measurements. Several configurations are tested and analyzed to study the influence of the arc current, the relative speed, the mode of relative motion (propelled test sample or arc blow) and of the test sample polarity on the phenomenon. A preliminary study has shown that the formation and the dwelling of an arc spot are governed by different physical processes for the anode and the cathode considering the plasma sheath. Then, the protocol to measure physical values that account for the mode of displacement – continuous or jumping – is described and the results are reported.

The results show that for the cathodic arc root displacement, the jumping mode is favored for lower values of relative speed between the arc and the sample and higher values of current. For the anodic arc root displacement, only a jumping mode is observed. A higher relative speed involves longer dwell times and longer portions of arc column extinguished during a reattachment. The influence of current is difficult to interpret. The mode of relative motion, RGE or WTE, does not present a difference comparing the orders of magnitude of the physical quantities involved in the swept-stroke. However, the variation of these quantities with the experimental conditions shows some marked differences between RGE and WTE: an increased relative speed between the test sample and the air flow provokes a jumping anodic arc root motion that is more prominent for RGE than for WTE.

These results represent a first contribution to the problem of the arc root displacement in the goal to understand the complex physical mechanisms that drive the swept-stroke phenomenon during a lightning strike to airborne vehicle. This works aims at being used as a comparative work for future experiments and computational simulations.

ACKNOWLEDGMENTS

The authors wish to thank the French Civil Aviation Authority (DGAC), France Relance and NextGenerationEU for their supports.

DATA AVAILABILITY

All data that support the findings of this study are included within the article (and any supplementary files).

REFERENCES

[1] Plumer J A 2012 *Int. Conf. on Lightning Protection (Vienna, Austria)*

[2] Chemartin L, Lalande P, Peyrou B, Chazottes A, Elias P Q, Delalondre C, Cheron B G and Lago F 2012 *J. Aerosp. Lab* AL05-09 (available at: http://aerospacelab.onera.fr/al5/direct-effects-of-lightning-on-aircraft-structureanalysis-of-the-thermal-electrical-and-mechanical-constraints)

[3] Xiangteng M, Fusheng W, Han C, Donghong W and Bin X 2020 *Chinese J. Aeronaut.*, **33** (4) 1242-51

[4] Sousa Martins R, Rivière P, Zaepffel C, Passilly F and Soufiani A 2020 *J. Appl. Phys.* **128** 223301

[5] Sousa Martins R 2016 Experimental and theoretical studies of lightning arcs and their interaction with aeronautical materials *PhD Thesis* Ecole Centrale Paris

[6] Tholin F, Chemartin L and Lalande P 2015 *Int. Conf. on Lightning and Static Electricity, Toulouse* (*France*)

[7] Xiao C and Liu Y 2023 *Front. Astron. Space Sci.* **10** 1083158 (doi: 10.3389/fspas.2023.1083158)

[8] Guerra-Garcia C, Nguyen N C, Peraire J and Martinez-Sanchez M 2016 *J. Phys. D: Appl. Phys.* **49** 375204

[9] Dobbing J A and Hanson A W 1978 *Int. Symp. On Electromagnetic compatibility* (*Atlanta*)

[10] Andraud V, Sousa Martins R, Zaepffel C, Landfried R, Testé and Lalande P 2023 *J. Phys. D: Appl. Phys.* **56** 395202

[11] McBride J W and Jeffery P A 1999 *IEEE Trans. Compon. Packag. Manuf. Technol*. **22** 38–46

[12] Yang G and Heberlein J V 2007 *J. Phys. D: Appl. Phys.* **40** 5649

[13] Freton P, Gonzalez J J and Escalie G 2009 *J. Phys. D: Appl. Phys.* **42** 195205

[14] Cui Y, Niu C, Wu Y, Zhu M, Yang F and Sun H 2017 *4th Int. Conf. on Electric Power Equipment-Switching Technology (ICEPE-ST)* (DOI: 10.1109/ICEPE-ST.2017.8188930)

[15] Gray M, Choi Y J, Sirohi J and Raja L L 2015 *J. Phys. D: Appl. Phys.* **49** 015202.

[16] Gray M, Choi Y J, Sirohi J and Raja L L 2018 *J. Phys. D: Appl. Phys.* **51** 315203

[17] Choi Y J, Gray M, Sirohi J and Raja L L 2017 *J. Phys. D: Appl. Phys.* **50** 355203

[18] Guile A E and Mehta S F 1957 *Proceedings of the IEE-Part A: Power Engineering* **104** 533-540

[19] Secker P E and Guile A E 1959 *Proceedings of the IEE-Part A: Power Engineering* **106** 311-320

[20] Boukhlifa M 2021 Contribution à l'étude des arcs électriques sur réseau HVDC (540 VDC) en conditions aéronautiques *PhD Thesis* Université Paris-Saclay

[21] Teste P, Leblanc T and Chabrerie J P 1995 *Journal of Physics D : Applied Physics* **28** 888.

[22] Andraud V, Sousa Martins R, Zaepffel C, Landfried R and Testé P 2021 *Rev. Sci. Instrum.* **92** 104709

[23] Andraud V, Sousa Martins R, Zaepffel C, Landfried R and Testé P 2022 *Rev. Sci. Instrum.* **93** 084705

[24] Eurocae ED-84, *Aircraft Lightning Environment and Related Test Waveforms Standard*, (2013).

[25] Andraud V 2022 Experimental implementation and study of the lightning swept-stroke along an aircraft *PhD Thesis* Université Paris-Saclay

[26] Sunabe K and Inaba T 1990 Electr. Eng. Japan **110** 9 (DOI: 10.1002/eej.4391100102)

[27] McBride J W and Jeffery P A 1999 *IEEE Trans. Compon. Packag. Manuf. Technol.* **22** 38–46

[28] Guile A E 1971 *Proceedings of the Institution of Electrical Engineers* **118** 9 1131-1154

[29] Froome K D 1948 *Proceedings of the Physical Society* **60** 424

[30] Murphy E L and Good Jr R H 1956 *Physical review* **102** 1464

[31] Fowler R H and Nordheim L 1928 *Proceedings of the Royal Society of London. Series A, Containing Papers of a Mathematical and Physical Character* **119**, 173-181

[32] Sommerville J M 1959 *The Electric Arc* (Methuen and Company, Ltd, London)

[33] Ecker G 1953 *Die Stabilisierung des Lichtbogens vor Anode und Kathode. Zeitschrift für Physik,* **136** 1-16

[34] Lee T H 1959 *J. Appl. Phys.* **30** 166-171